

# Simulations of galaxy formation and evolution

C. Scannapieco\*

Leibniz-Institut für Astrophysik Potsdam (AIP), An der Sternwarte 16, D-14482 Potsdam, Germany

Received 2012 Jan 19, accepted 2012 Apr 10

Published online 2012 Jun 15

**Key words** galaxies: formation – galaxies: evolution – cosmology: theory – methods: numerical

We discuss recent results of hydrodynamical simulations of galaxy formation in a  $\Lambda$  Cold Dark Matter universe, focusing on galaxies of similar mass to the Milky Way, and with a variety of formation and merger histories. We investigate the present-day properties of disks and spheroids, in terms of stellar ages, spatial structure and dynamics; as well as the evolution of the disks. We find that disks are young, and usually composed of two or more components: the youngest stars define thinner disks that rotate  $\sim 2$  times faster than thicker disks. The latter are populated by older stars, and have 2–3 times larger velocity dispersions than the younger population. Spheroids are old and are very diverse; their inner regions are sometimes characterized by the presence of prominent bars. The disks evolve significantly during evolution. In particular, we find that major mergers and misaligned gas accretion are able to completely or partially destroy disks. These results suggest that the survival probability of disks, and therefore the final morphology of galaxies, strongly depends on the particular formation and merger history of their parent haloes. Our results show that galaxy diversity arises naturally in  $\Lambda$ CDM as a result of the different evolutionary paths of dark matter haloes. We also discuss the most important open problems in this field.

© 2012 WILEY-VCH Verlag GmbH & Co. KGaA, Weinheim

## 1 Introduction

Galaxies are very diverse objects. Their star formation histories, sizes, morphologies, gas content, show variations that are as high as an order of magnitude, even for a given stellar mass. Understanding how galaxies form, and how such variety of galaxy properties arises during their evolution, is one of the primary goals of modern astrophysics.

According to the current cosmological paradigm, the  $\Lambda$  Cold Dark Matter ( $\Lambda$ CDM) model, galaxies form hierarchically: small systems form first and larger systems form later via aggregation of smaller substructures and mergers. Galaxies thus follow unique evolutionary paths, being affected by the particular merger, accretion and formation history. The diversity in galaxy properties is then expected to be a natural outcome of the  $\Lambda$ CDM scenario.

Hydrodynamical simulations are a powerful tool to study galaxy formation in the context of a cosmological model. However, due to the huge dynamical range they need to cover, this type of simulations is currently not able to include processes such as star formation and feedback from first principles, since these act at scales that are not resolved. Modern simulation codes include these processes as sub-grid physics, which lead to the emergence of a number of alternative approaches (e.g. Springel & Hernquist 2003; Okamoto et al. 2005; Scannapieco et al. 2005, 2006; Rasera & Teyssier 2006; Stinson et al. 2006). Even if these do not always converge to the exact same result (see, e.g., Scannapieco et al. 2012), they have shown to be very powerful

to identify the effects of different physical processes on the evolution of galaxy properties.

Perhaps the most clear example of how simulations can help us understand galaxy formation is related to the well-known *angular momentum problem*. This is a common problem in simulations that do not include feedback, which happens as baryons transfer a significant amount of their initial angular momentum to the dark matter component during mergers and interactions (Navarro & Benz 1991; Navarro & Steinmetz 2000). As a result, it has been very difficult to produce realistic disk galaxies in dark matter haloes formed hierarchically (e.g. Navarro et al. 1995; Navarro & Steinmetz 1997). More recent simulation codes including feedback processes, in particular from SN explosions, have shown to be successful in reproducing disk-like systems, suggesting that feedback processes are indeed a crucial ingredient in galaxy formation (e.g., Governato et al. 2004, 2007; Okamoto et al. 2005; Scannapieco et al. 2008, 2009; Ceverino & Klypin 2009; Stinson et al. 2010). SN feedback, through the return of energy and mass to the interstellar medium, is efficient in regulating star formation, preventing overcooling and helping baryons to retain their angular momentum (e.g. Navarro & Steinmetz 1997; Scannapieco et al. 2008).

In this paper, we use eight simulations of the formation of galaxies in a  $\Lambda$ CDM universe. These simulations were first presented in Scannapieco et al. (2009) and correspond to galaxies similar in mass to the Milky Way, and with a variety of formation and merger histories. This sample allows us to investigate the most relevant processes shaping the properties of galaxies as they evolve.

\* Corresponding author: cscannapieco@aip.de

This paper is organized as follows. Section 2 describes the simulation code, initial conditions and cosmological parameters; Sect. 3 explores the properties of the disks and spheroids formed in our simulations; and Sect. 4 discusses the evolution of the disks and the effects of mergers and accretion on the morphologies of galaxies. Finally, in Sect. 5 we discuss a number of open problems in this field and in Sect. 6 we summarize our conclusions.

## 2 Methodology

We use cosmological, hydrodynamical simulations to investigate the formation process of galaxies similar in mass to our Milky Way. In particular, the results discussed here correspond to the simulations presented in Scannapieco et al. (2009) and extensively described in Scannapieco et al. (2009, 2010, 2011). Additional papers describe the effects of baryons on the dark matter distributions (Tissera et al. 2010) and the chemical patterns of simulated galaxies (Tissera, White & Scannapieco 2012). The following sections describe the basics of the simulations: the initial conditions, the simulation code and the included physical processes.

### 2.1 The simulation code

We use the simulation code described in Scannapieco et al. (2005) and Scannapieco et al. (2006). It is a GADGET-based code (Springel 2005; Springel et al. 2008) that combines a Tree-PM solver for the computation of gravitational forces with the Smoothed Particle Hydrodynamics (SPH) technique to solve the gas dynamics. This model includes stochastic star formation, metal-dependent cooling, a multiphase model for the gas component, and chemical and energy feedback from type II and type Ia supernova (SN) explosions.

The multiphase model allows hot, diffuse gas to coexist with a cold, dense gas phase, and helps to make the deposition of SN energy into the interstellar medium more efficient, avoiding artificial losses usually occurring in standard SPH implementations of thermal feedback. This implementation is fully independent of that of Springel & Hernquist (2003) but uses their treatment of a UV background, based on the work of Haardt & Madau (1996).

The model is currently grafted into GADGET3 (Springel et al. 2008), the most recent version of the GADGET code. For more details on the simulation code, we refer the reader to Scannapieco et al. (2005, 2006). The code has been already applied to the study of Milky Way-mass galaxies (Scannapieco et al. 2008, 2009, 2010, 2011), as discussed in this paper, and to the study of dwarf galaxies (Sawala et al. 2010, 2011).

### 2.2 The simulations

The simulations discussed here correspond to hydrodynamical simulations in a cosmological context. They use the

**Table 1** Main properties of our simulated halos at  $z = 0$ : virial mass, mass in stars, mass in gas, and optical radius.

Halo	$M_{200}$ [ $10^{11}M_{\odot}$ ]	$M_{\text{star}}$ [ $10^{10}M_{\odot}$ ]	$M_{\text{gas}}$ [ $10^{10}M_{\odot}$ ]	$r_{\text{opt}}$ [kpc]
Aq-A-5	14.9	9.0	4.6	17.9
Aq-B-5	7.1	4.0	1.7	17.7
Aq-C-5	16.1	10.8	3.6	16.0
Aq-D-5	14.9	7.9	3.2	14.8
Aq-E-5	10.8	8.4	2.6	10.6
Aq-F-5	9.1	7.7	1.7	14.1
Aq-G-5	6.8	4.4	1.53	14.1
Aq-H-5	7.4	6.5	0.52	10.4

zoom-in technique, which allows to describe the formation of a galaxy and its surroundings with very high-resolution, keeping the information on the larger scales. This is done by using different hierarchies of particles whose mass resolution is decreased as they are further away from the target galaxy.

The initial conditions are based on those of the Aquarius Project (Springel et al. 2008), and correspond to eight galaxies that, at  $z = 0$ , have a similar mass to the Milky Way. They have been selected randomly from the parent dark-matter only simulation, the Millennium-II run (Boylan-Kolchin et al. 2009), with the only condition (additionally to the virial mass of the halo) of being mildly isolated (no neighbour exceeding half its mass within 1.4 Mpc). Table 1 shows the virial masses, the masses in stars and gas, and the optical radii (the radius enclosing 83 % of the baryonic mass) of our simulated galaxies.

The simulations are consistent with a  $\Lambda$ CDM cosmology with  $\Omega_{\Lambda} = 0.75$ ,  $\Omega_{\text{m}} = 0.25$ ,  $\Omega_{\text{b}} = 0.04$ ,  $\sigma_8 = 0.9$  and  $H_0 = 73 \text{ km s}^{-1} \text{ Mpc}^{-1}$ . The eight simulations have similar dark matter and gas particle masses, of  $\sim 10^6 M_{\odot}$  and  $\sim 3 \times 10^5 M_{\odot}$ , respectively. We have used similar gravitational softenings, either 0.7 or 1.4 kpc, which is the same for gas, stars and dark matter particles (see Scannapieco et al. 2009 for details).

## 3 Galaxies at $z = 0$

In this section we describe the properties of simulated galaxies at  $z = 0$ . In particular, their morphologies, stellar populations, spatial structure and dynamical properties.

### 3.1 Morphologies and the disk-spheroid decomposition

The eight simulated galaxies show, at  $z = 0$ , a variety of morphologies, as can be seen in Fig. 1, where we show maps of projected stellar luminosity in the  $i$ -band (Scannapieco et al. 2010). Clearly, the simulated galaxies have very different shape and spatial extent, partly due to their different virial masses, but more importantly, due to their different formation and merger histories.

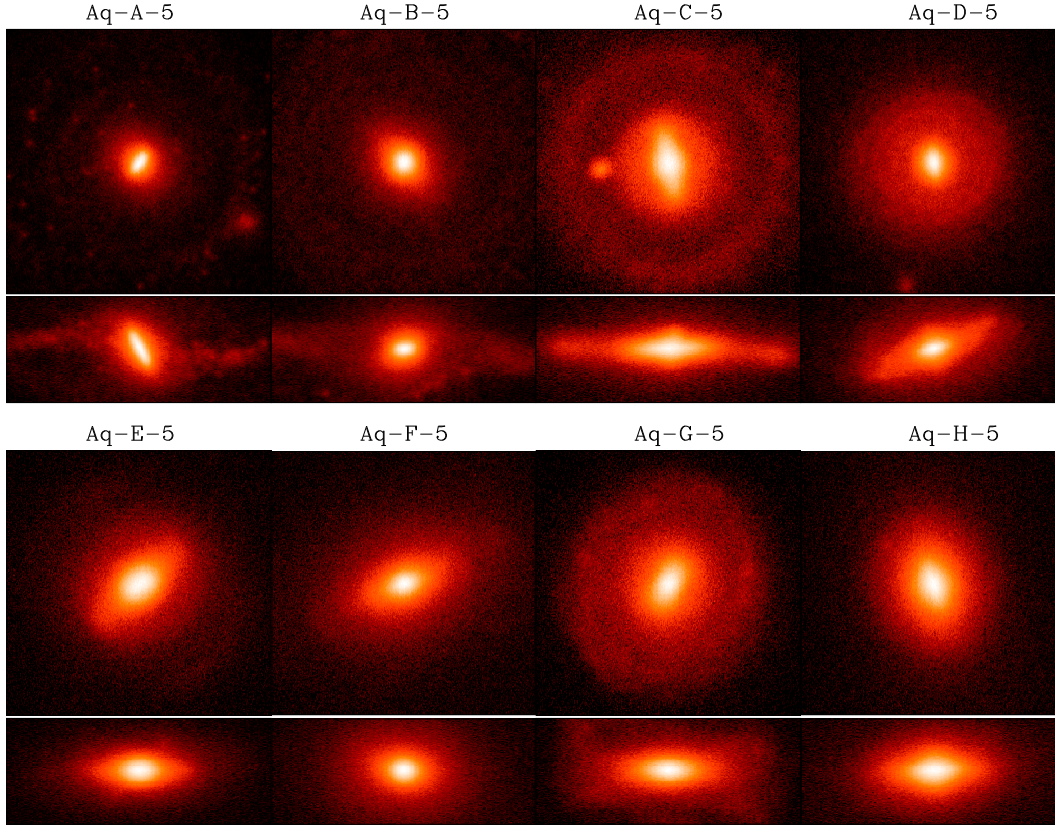


**Fig. 1** Face-on and edge-on maps of projected stellar luminosity ( $i$  band) for our simulations, at  $z = 0$ . The images are 50 kpc across, and the edge-on ones have a vertical height of 20 kpc (Scannapieco et al. 2010).

In order to quantify the morphology of the galaxies and to study the properties of disks and spheroids separately, we use a disk-spheroid decomposition based on the kinematics of the stars. Our method is explained in detail in Scannapieco et al. (2009); here we only describe its main characteristics. The starting point is the calculation of the stellar *circularities*, defined as

$$\epsilon \equiv \dot{j}_z / \dot{j}_{\text{circ}}, \quad (1)$$

where  $\dot{j}_z$  is the angular momentum of each star in the  $z$  direction (i.e. the direction of the total baryonic angular momentum) and  $\dot{j}_{\text{circ}}$  is the angular momentum corresponding to a circular orbit at the position of the star. Values of  $\epsilon$  similar to unity identify stars with disk-like kinematics. These are then tagged as disk stars, while the remaining stars define the spheroidal component. Note that spheroids then include bulge and stellar halo stars, but also stellar bars when these are present. Section 5.2 presents a discussion on advantages and disadvantages of using kinematic methods, and compares results obtained with methods used in observations.

Figure 2 shows the distribution of stellar circularities of our simulations. All galaxies show a significant spheroidal component. In all cases except Aq-E-5, the spheroid is not rotating, as inferred from the fact that the distribution peaks at  $\epsilon \sim 0$ . In Aq-E-5, the spheroid is clearly rotating. We

find that all except one galaxy have disk components, and that the disk prominence varies significantly from galaxy to galaxy. In particular, four of the eight galaxies, namely Aq-C-5, Aq-D-5, Aq-E-5 and Aq-G-5, have prominent disks. In contrast, Aq-A-5, Aq-B-5 and Aq-H-5 have very small disk components. Aq-F-5 has no disk: this feature can be attributed to a recent major merger that fully destroys a pre-existing disk, as will be discussed in Sect. 4.

The disk-spheroid decomposition allows to calculate disk-to-total ratios for the simulated galaxies, since each star belongs to either the disk or the spheroidal component. Table 2 shows the (mass-weighted) disk-to-total ratios ( $D/T^k$ ) obtained with the kinematic approach. The maximum  $D/T$  ratios are about 0.2, and are too small to be compatible with disk-dominated galaxies. However, as discussed in Sect. 5.2, it is not meaningful to directly compare our  $D/T^k$  with  $D/T$  ratios obtained from observations. In fact, when using methods identical to those used in observations, our simulated galaxies have  $D/T$  ratios that are significantly larger than those obtained with the kinematic decomposition (Sect. 5.2).

### 3.2 Stellar ages

In this section, we investigate the ages of stars in the disk and the spheroidal components. Because spheroid stars ex-

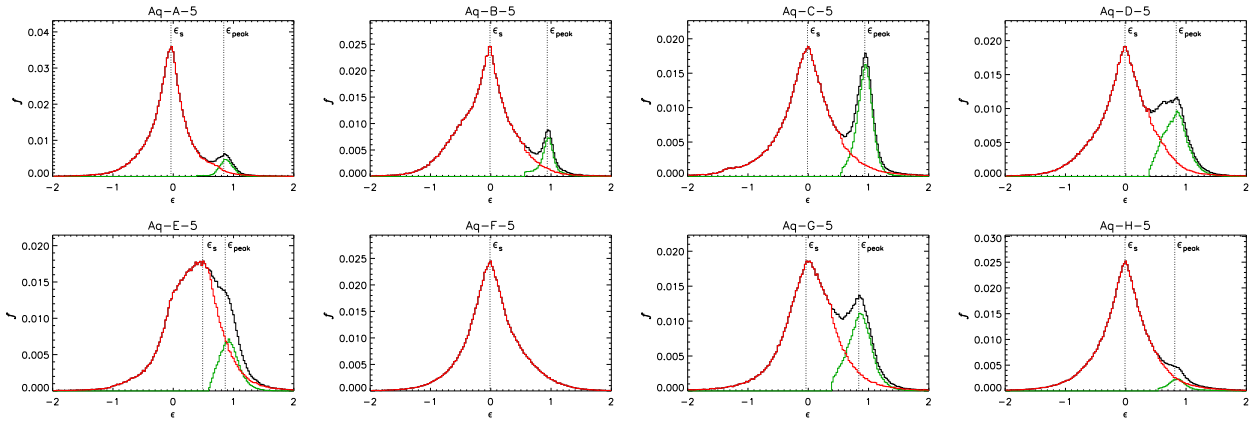


**Fig. 2** (online colour at: [www.an-journal.org](http://www.an-journal.org)) Stellar mass fraction as a function of  $\epsilon = j_z/j_{\text{circ}}$  for our set of simulations at  $z = 0$  (black lines). Red and green lines correspond to the distributions for spheroid and disk stars, respectively, obtained with our disk-spheroid decomposition (Scannapieco et al. 2009).

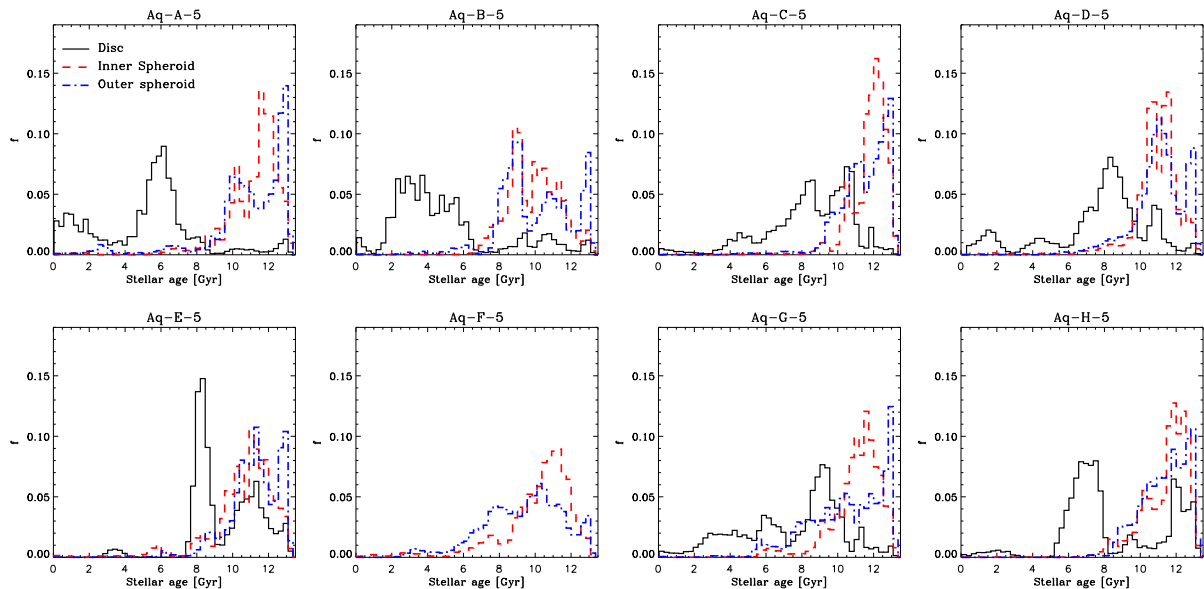


**Fig. 3** (online colour at: [www.an-journal.org](http://www.an-journal.org)) Distribution of (mass-weighted) stellar ages for the disk (solid lines), inner spheroid (dashed lines) and outer spheroid (dotted-dashed lines) components in our simulations. For clarity, each component has been normalized to its total mass (Scannapieco et al. 2009).

tend all the way to the virial radius (although the vast majority are in the central regions), we subdivide the spheroids into “inner” ( $r \leq r_{\text{opt}}$ ) and “outer” ( $r > r_{\text{opt}}$ ) components ( $r_{\text{opt}}$  is the radius which encloses 83 % of the baryonic galaxy mass, see Table 1).

Figure 3 shows the distribution of stellar ages for the disks, inner spheroids and outer spheroids, for our eight simulations. In all cases, the disks are the youngest components, while inner and outer spheroids are composed mainly of old stars. We detect no systematic difference between the stellar age distributions of inner and outer spheroidal components. In the case of the disks, we find superposition of stars of different ages, perhaps indicative of thin and thick disks, as we discuss below.

Mean stellar ages are in the range 9–12 Gyr for spheroids and 4–9 Gyr for disks. These are mass-weighted quantities, while in observations luminosity-weighted ages are instead obtained. We have calculated luminosity-weighted mean stellar ages for our simulations, using the Bruzual & Charlot (2003) population synthesis models. In this way, we obtain luminosity-weighted mean ages of 10–12 Gyr and 2–8 Gyr for the spheroids and disks, respectively. These values are very similar to the mass-weighted estimates for spheroids but, due to their younger ages, they are significantly lower for disks. The mean ages of our disks and spheroids are in relatively good agreement with observational results: observations find typical mean ages of

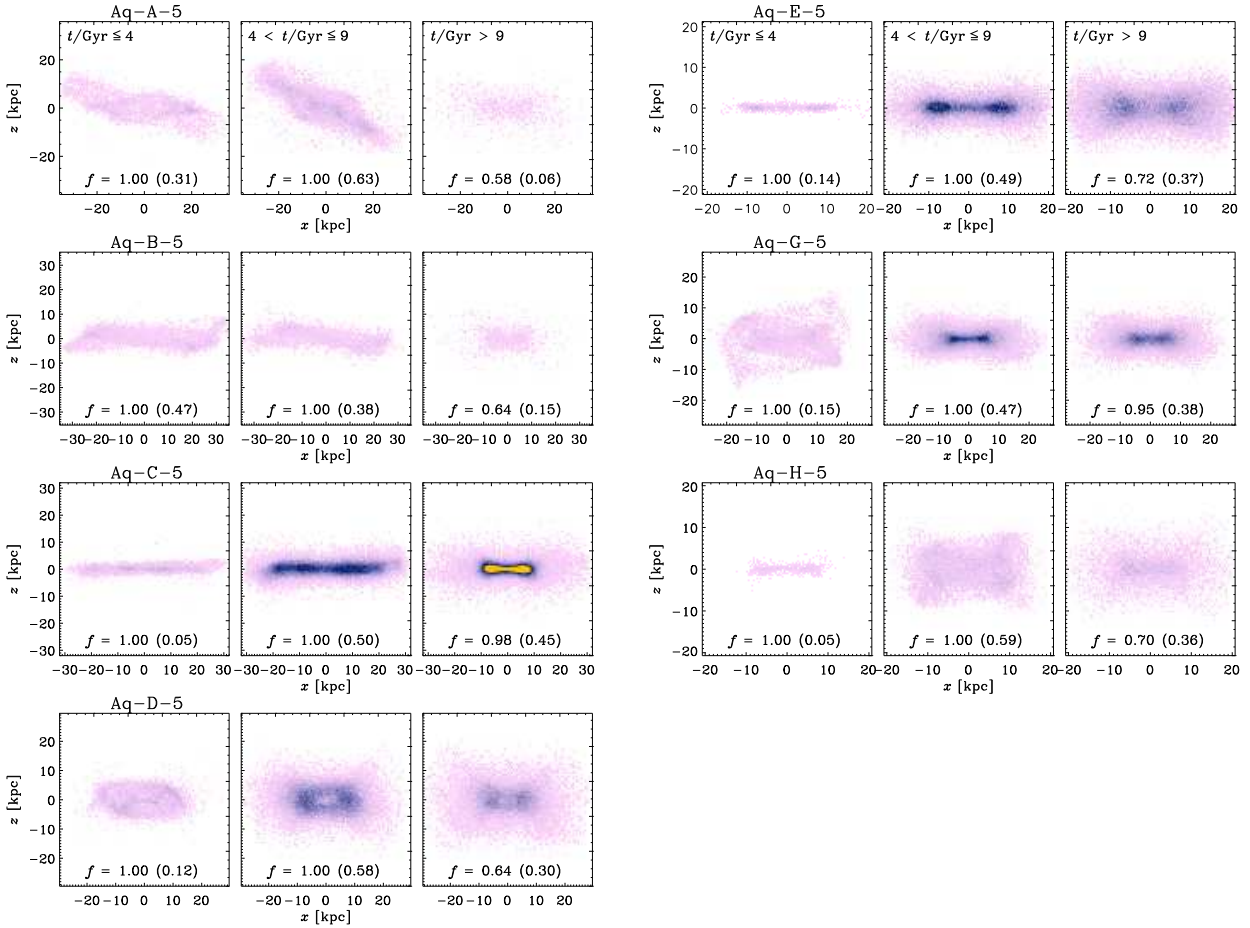


**Fig. 4** Spatial distribution of disk particles (up to twice the corresponding optical radius) for the simulations with a disk component. We show separately the distribution of young stars ( $t \leq 4$  Gyr), intermediate age stars ( $4 < t \leq 9$  Gyr), and old stars ( $t > 4$  Gyr) in the disks. Colours represent surface mass density, and cover 4 orders of magnitude ( $10^4$ – $10^8 M_{\odot} \text{ kpc}^{-2}$ ). We also show the *in-situ* fraction of disk stars for the three stellar age bins, together with the corresponding disk mass fraction (in parentheses). (Scannapieco et al. 2011).

**Table 2** Results from the kinematic and photometric decompositions of the eight simulated galaxies: we show the disk-to-total ratios obtained with the kinematic and photometric approaches, and the bulge-to-total and bar-to-total ratios of the latter method. Results in parenthesis correspond to galaxies for which the photometric decomposition did not give a reliable result.

Galaxy	D/T <sup>k</sup>	D/T <sup>P</sup>	B/T <sup>P</sup>	Bar/T <sup>P</sup>
Aq-A-5	0.06	0.32	0.45	0.23
Aq-B-5	0.09	0.42	0.58	-
Aq-C-5	0.21	0.49	0.28	0.23
Aq-D-5	0.20	0.68	0.32	-
Aq-E-5	0.14	0.40	0.17	0.43
Aq-F-5	-	(0.44)	(0.56)	-
Aq-G-5	0.23	0.60	0.06	0.34
Aq-H-5	0.04	(0.05)	(0.95)	-

bulges and disks of  $>8$  Gyr and 4–12 Gyr, respectively (MacArthur et al. 2004, 2009).

The stellar age distributions can also be used to estimate the typical formation time-scales of the different components, simply from the values of the standard deviation. As is evident from Fig. 3, disks form over larger time-scales, with  $\Delta\tau$  values between 2 and 3 Gyr. In contrast, the formation time-scales of spheroids are small, typically in the range 1–2 Gyr.

### 3.3 Spatial and dynamical structure

We now discuss the structure of simulated disks and spheroids, in terms of spatial distribution and dynamical properties. Figure 4 shows the distribution of disk particles, in an edge-on view, of our simulations (note that Aq-F-5 has no disk). We plot separately stars formed in three different age bins:  $t/\text{Gyr} \leq 4$ ,  $4 < t/\text{Gyr} \leq 9$  and  $t/\text{Gyr} > 9$ . The plots are color-coded according to the surface mass density at each point; covering 4 orders of magnitude ( $10^4$ – $10^8 M_{\odot} \text{ kpc}^{-2}$ ).

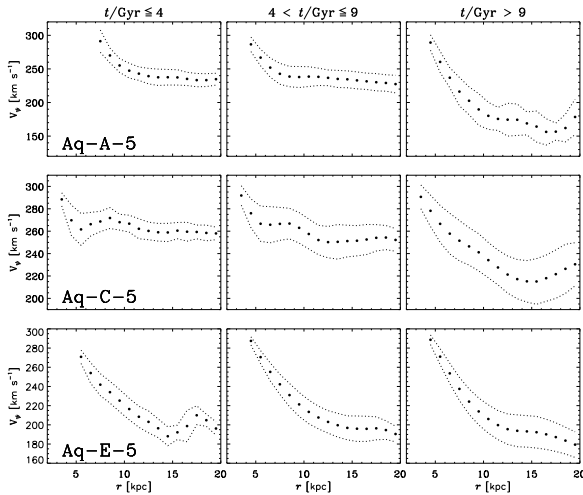


**Fig. 5** Mean tangential velocity of disk stars as a function of projected radius in the disk plane (filled circles) for Aq-A-5, Aq-C-5 and, Aq-E-5. The width between the dotted lines is the tangential velocity dispersion (Scannapieco et al. 2011).

We find that a few of the simulated disks are very thin (Aq-C-5, Aq-E-5) but we also detect a great variety: we find “boxy” or “X”-shaped disks (Aq-D-5, Aq-G-5, Aq-H-5), warps (Aq-B-5), and a case where two misaligned disks of different age are present (Aq-A-5). In all cases, however, we find that the youngest stars define thinner disks than stars in the older age bins.

Stars of different age also present different dynamical properties. As an example, we show in Fig. 5 the mean tangential velocity of disk stars as a function of projected radius for Aq-A-5, Aq-C-5 and Aq-E-5 and the corresponding velocity dispersion. (The results for the other runs are similar, see Scannapieco et al. 2011.) In all cases, the youngest components of the disks rotate  $\sim 2$  times faster and have 2–3 times lower velocity dispersions than the older disk components. These results are indicative of the presence of young, thin components together with older and thicker disks; as also found in spiral galaxies.

Spheroids are also found to be very diverse, specially in their inner regions. Figure 6 shows maps of surface mass density for simulated inner spheroids (up to  $0.5 \times r_{\text{opt}}$ ). Inner spheroids have bulge-like components that are very diverse in shape: some are almost axisymmetric, others are strongly ellipsoidal. Furthermore, some of the simulated galaxies, such as Aq-C-5 and Aq-G-5, have prominent bars (Scannapieco & Athanassoula, in prep.).

Figure 7 shows the profiles of radial, tangential and vertical velocities for spheroid stars, as well as the corresponding total velocity dispersions. For the vertical velocities, we use  $V_z^* \equiv V_z \text{sign}(z)$ , in order to distinguish between inflows ( $V_z^* < 0$ ) and outflows ( $V_z^* > 0$ ). We find very small radial and vertical velocity components in all simulations. In some cases, there are signs of non-zero but small radial velocities in the outermost regions, but these are not significant, specially taking into account that the amount of stellar

mass in these regions is very small. We do find non-zero tangential velocities with a great variety of patterns: Aq-A-5 and Aq-B-5 are counter-rotating in the inner parts and co-rotating in the outer regions (always in relation to the overall rotation of the disk); the spheroidal component of Aq-E-5 has a net rotation (Scannapieco et al. 2009, 2011); the other galaxies show signs of co-rotation, mainly outside the inner regions. The total velocity dispersions decline with radius, varying typically from 150–250  $\text{km s}^{-1}$  in the inner regions to 50–100  $\text{km s}^{-1}$  near the virial radius.

The diversity in the structure of galaxies arises naturally in our simulations, as a consequence of the variety of formation, merger and accretion histories in the context of the  $\Lambda$ CDM cosmological model.

## 4 Evolution

In this section we discuss how the morphology of our simulated galaxies evolve, and which are the most important processes inducing morphological transformations. Figure 8 shows the evolution of the disk-to-total ratio (obtained using our kinematic method) for our eight simulations. Arrows indicate the entrance of satellites (see caption for color code), while the red points indicate periods of strong misalignment between the gas and stellar disks.

This figure nicely illustrates a number of features: (i) most galaxies have prominent disks at high redshift ( $z \sim 2-3$ ); (ii) the disk-to-total ratios significantly change between  $z = 3$  and  $z = 0$ ; (iii) the morphology of a galaxy can change in very short time-scales.

Major mergers are known to affect the morphology of galaxies; being able to convert disks into spheroids. In our eight galaxies, and between  $z = 3$  and  $z = 0$ , we detect only one major merger event ( $M_{\text{sat}}/M_{\text{central}} > 0.3$ ), that occurs in Aq-F-5 at  $z \sim 0.5$ . After the merger, the D/T ratio decreases from 0.3–0.4 to 0 very quickly, indicating that the merger fully destroyed the disk component.

Another possible mechanism to induce morphological transformations is a misalignment between the gas and stellar disks. We investigated this process and calculated the angle between the angular momentum of the pre-existing stellar disk and the angular momentum of the gas disk. In fact, we find a correlation between the alignment of infalling gas with respect to the stellar disk and the evolution of the D/T ratio. If infalling gas is misaligned with the stellar disks, the D/T ratios inevitably decrease, as indicated by the red dots in Fig. 8. During these periods, disks become unstable: in some cases, such as Aq-A-5, Aq-B-5 and Aq-H-5, disks are almost completely destroyed; in others, disks survive (Aq-E-5). Note that the disk in Aq-A-5 was one of the most prominent disks of all simulations at  $z \sim 1$ ; when the misalignment starts, the D/T ratio decreases from  $\sim 0.6$  to 0.1. In Aq-D-5, the disk is destroyed but a new disk grows significantly at recent times.

Finally, we find that minor merger events can also affect disks, but their effects depend on other properties such as

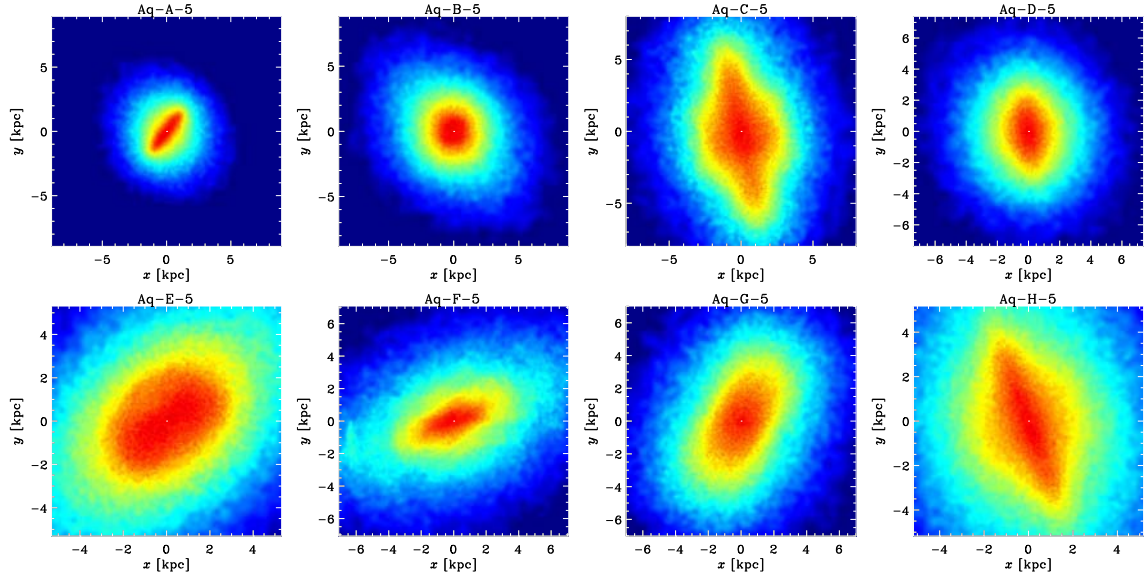


**Fig. 6** Spatial structure of simulated inner spheroids, up to  $0.5 r_{\text{opt}}$ . The projection is face-on, such that the disks are contained in this plane. Colors represent projected surface mass density, on a logarithmic scale that covers 2.5 orders of magnitude (Scannapieco et al. 2011).

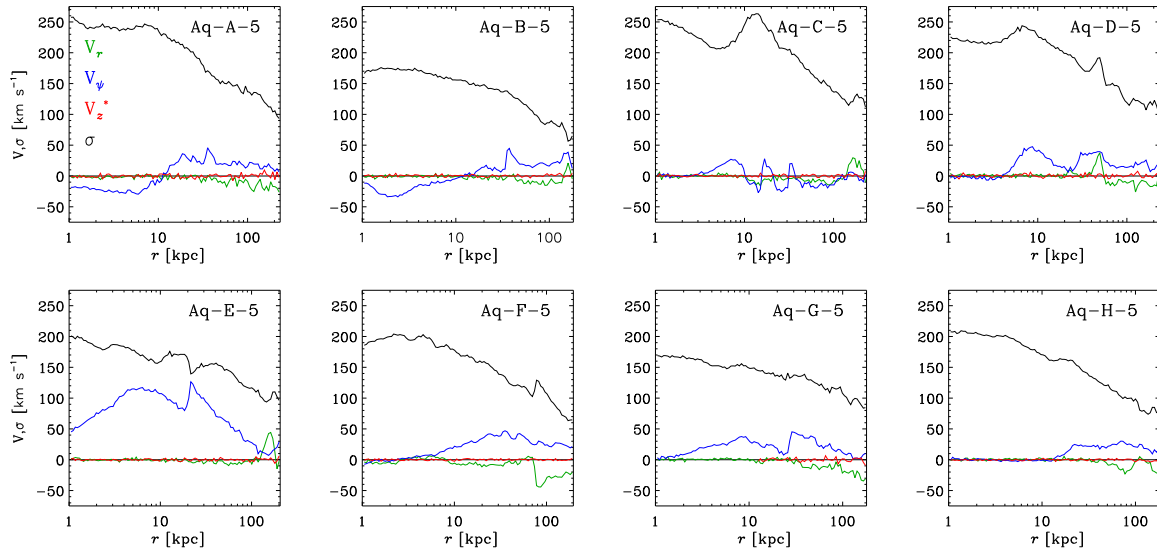


**Fig. 7** Radial (green), tangential (blue) and vertical (red) velocities as a function of projected radius for the spheroidal components of our simulated galaxies (up to the corresponding virial radii). In the case of the vertical velocities, we use  $V_z^* \equiv V_z \text{sign}(z)$ , in order to distinguish between inflows ( $V_z^* < 0$ ) and outflows ( $V_z^* > 0$ ). We also show the profiles of total stellar velocity dispersion (black lines). (Scannapieco et al. 2011).

the satellite's orbit. In most cases of minor merger events, we find only little effects on the D/T ratios of simulated galaxies. However, in Aq-G-5, a minor merger is able to partially destroy the disk, lowering the D/T ratio from  $\sim 0.45$  to 0.2 in a very short time.

## 5 Discussion

In this section we discuss some problems and open questions of galaxy formation simulations in a cosmological

context. In particular, we focus on problems related to the massive spheroids found in most simulations; on difficulties in comparing disk-to-total ratios of simulated galaxies with observational results; on limitations of current simulations in relation to their high computational cost; and on differences in the predictions of galaxy properties when various codes are used.

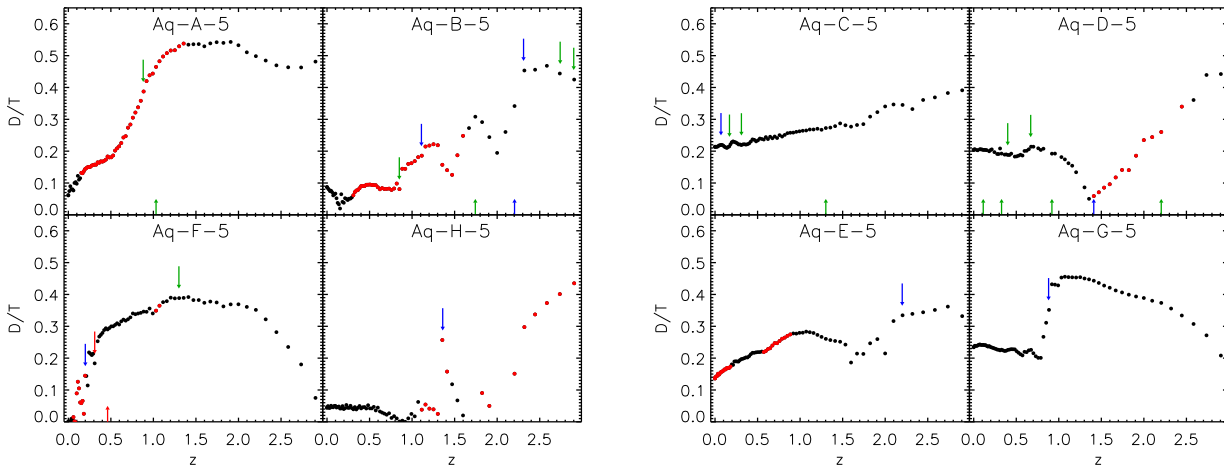


**Fig. 8** (online colour at: [www.an-journal.org](http://www.an-journal.org)) Kinematic disk-to-total mass ratio as a function of redshift for simulated galaxies. We have divided the plot in such a way that galaxies with little or no disk components at  $z = 0$  are plotted in the left-hand panel, while galaxies with more prominent disks at the present time reside in the right-hand one. The arrows indicate the entrance of satellites either to the virial radius (upward arrows) or to the central (comoving) 27 kpc (downward arrows). Arrows are colour-coded according to the merger ratio  $f \equiv M_{\text{sat}}/M_{\text{cen}}$ : red, blue and green colours correspond to  $f > 0.3$ ,  $0.1 < f \leq 0.3$ , and  $0.02 < f \leq 0.1$ , respectively. Red points indicate periods of strong misalignment between the cold gaseous and stellar disks (Scannapieco et al. 2009).

### 5.1 Disks versus spheroids - Feedback modelling

During the last decade, significant progress has been done in the study of disk formation from cosmological initial conditions. In particular, the inclusion of efficient models of feedback processes showed that the angular momentum problem can be alleviated when feedback is included, and that disks with sizes comparable to those of observed galaxies can be obtained. However, in most simulations massive spheroids form very early on, and the galaxies are, at  $z = 0$ , dominated (in mass) by compact bulges. As a result, it seems difficult to obtain galaxies with very small bulges or bulge-less galaxies.

Currently, models with strong SN feedback, even if obtaining massive bulges in addition to the disks, seem the most successful in reproducing a number of observational results (see Scannapieco et al. 2012); although there is still debate on this topic. Moreover, a number of works have shown that varying the feedback model, or varying the input parameters of a given implementation, can lead to different final morphologies, even for a given halo (e.g. Okamoto et al. 2005; Scannapieco et al. 2008).

It has also been suggested that weak feedback models, together with low star formation efficiency, are more likely to produce disk-like morphologies (e.g. Agertz et al. 2011), although these models tend to obtain galaxies with too high stellar mass (Scannapieco et al. 2012). Furthermore, some authors have claimed that increasing the numerical resolution (e.g. Governato et al. 2007) or varying the cosmological model to Warm Dark Matter models (e.g. Mayer, Governato & Kaufmann 2008), might also help to produce galaxies more similar to those observed.

### 5.2 Disk-bulge decompositions and the D/T ratio

Another complication of studies with simulations is related to the need to compare them with observations in a meaningful manner. For example, we have shown that, in our simulations, the D/T ratios obtained using kinematic methods are very small in comparison with those of spirals (see also Stinson et al. 2010).

Scannapieco et al. (2010) investigated whether the kinematic disk-spheroid decompositions usually used in simulation studies can be directly compared to the results of photometric decompositions, as done in real observations. To this end, we first produced synthetic images of the simulated galaxies using the radiative transfer code SUNRISE (Jonsson 2006). The images were then analysed using the BUDDA code (Gadotti 2008), that performs bulge-disk-bar decompositions to observed images. The results of this photometric decomposition are shown in Table 2, where we list the disk-, bulge-, and bar-to-total ratios ( $D/T^{\text{P}}$ ,  $B/T^{\text{P}}$  and  $\text{Bar}/T^{\text{P}}$ , respectively). The D/T ratios obtained in this way are significantly larger than those given by the kinematic decomposition (see Scannapieco et al. 2010 for a detailed discussion on the reasons of such differences).

A meaningful comparison between simulations and observations is crucial to identify agreement or disagreement between them; and simply comparing kinematic and photometric disk-to-total ratios is probably not indicative of the similarity of simulated and observed galaxies (see also Abadi et al. 2003; Governato et al. 2007).

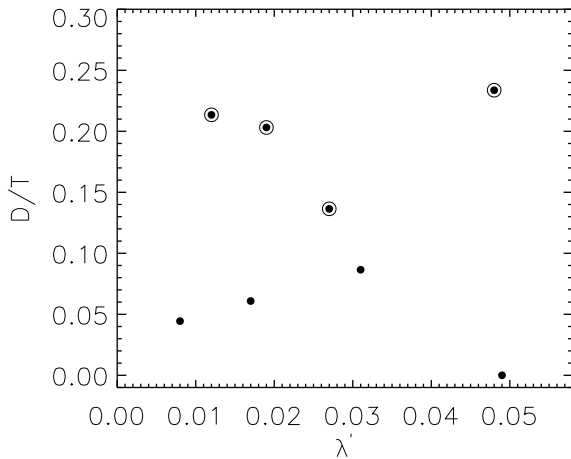


**Fig. 9** Disk-to-total mass ratio for our simulated galaxies as a function of the spin parameter of their parent haloes. Encircled symbols correspond to galaxies with well-formed disk components at  $z = 0$  (Aq-C-5, Aq-D-5, Aq-E-5 and Aq-G-5).

### 5.3 Simulating a representative sample of galaxies

High-resolution simulations such as the ones discussed here are computationally expensive. This has prevented the simulation of large numbers of galaxies in a cosmological context, preventing the exploration of galaxy properties and their evolution on a statistically significant number of systems. In  $\Lambda$ CDM, however, haloes are very diverse in terms of their merger, accretion and formation histories, which would translate into a huge variety of galaxies, even for a given halo mass.

A few recent studies have been able to simulate 8-10 galaxies in its full cosmological context (Brooks et al. 2009; Scannapieco et al. 2009; Stinson et al. 2010); opening up the possibility to investigate the variety of galaxy properties. Moreover, they allowed to study important relations such as the one between the morphology of a galaxy (usually quantified by the D/T ratio) and the spin parameter of its host halo ( $\lambda'$ ). Figure 9 shows this relation for the eight simulated galaxies discussed in this work. Although it is usually assumed that the galaxies with higher spin parameters have larger D/T ratios, we find no clear correlation between them. A similar result is found by Stinson et al. (2010) in their simulations.

Our results show that our knowledge on galaxy formation is still quite limited, and that the final relative prominence of disks and spheroids is determined by a complex interplay between internal processes such as cooling and feedback, and the particular accretion and merger history of a halo.

### 5.4 Comparison of different simulation codes

Another important problem in hydrodynamical simulations of galaxy formation is that different simulation codes usu-

ally produce a variety of results. Although this is an important test for simulations, little effort has been invested in detailed comparisons of the predictions of different models and in understanding the origin of any differences. Moreover, due to the inhomogeneity of initial conditions, implementation techniques, included physics, selection of input parameters and analysis tools, it is impossible to compare the successes of different codes in an unbiased manner from published studies. The lack of systematic comparisons between models make it unclear how robustly galaxy properties can be predicted by hydrodynamical simulations in general.

The Aquila Project (Scannapieco et al. 2012) has been designed to overcome these problems. We used a unique initial condition and an homogeneous set of analysis tools, and simulated the formation of a single dark matter halo in a  $\Lambda$ CDM universe using 13 different codes. These include both SPH and Adaptive Mesh Refinement (AMR) codes, and also a variety of physical processes.

Despite the common halo assembly history, we find large ( $\sim 1$  dex) code-to-code variations in the stellar mass, size, morphology and gas content of the galaxy at  $z = 0$  that result mainly from different implementations of feedback. During the next years, we expect to have both higher resolution and more sophisticated feedback models, which will probably help to better understand the formation of disks in a cosmological framework.

## 6 Conclusions

We have used a set of simulations to show the current status of hydrodynamical simulations of galaxy formation in a cosmological context. We used the sample first presented in Scannapieco et al. (2009), that focusses on galaxies of mass similar to our Milky Way and in a relatively quiet environment, and explored their  $z = 0$  properties and the evolution in their morphologies. The main successes of our simulations can be summarized as follows:

- (i) Disks can form from cosmological initial conditions, and current models including SN feedback efficiently prevent the angular momentum problem suffered by early simulations.
- (ii) A number of properties of disks and bulges can be reproduced by the simulations: bulges are formed mainly by old stars, over short time-scales, while disks are young and form over longer time-scales. Disks are better described by a superposition of more than one component: old disk stars rotate slower and have higher velocity dispersions than young disk stars. This result suggests the presence of thin and thick disk components in most simulated galaxies, similar to observational results.
- (iii) The simulated galaxies are very diverse in terms of their structure, dynamics and stellar populations. This diversity arises naturally in the context of  $\Lambda$ CDM, and is also observed in real galaxies. Future simulations will probably focus on the simulation of larger samples of galax-

ies, such that better comparison with observations can be made.

- (iv) The morphology of a galaxy can significantly change during evolution, and this evolution is mainly driven by the particular merger and accretion history of the haloes. We find that, additionally to major mergers that efficiently destroy disks, misalignment between the stellar disks and infalling gas strongly affects the disk-to-total ratios. Such misalignments are common during galaxy formation, and are able to partially or fully destroy disks.

Our results, and in particular, the successes explained above, are similar to those found by other works. There are, however, a number of open problems. In particular, most simulations find too massive spheroids, unless star formation is prevented at high redshift.

We have also shown that kinematic decompositions of simulated galaxies into disk and spheroidal components usually give too low D/T values compared to those observed in late-type spirals. However, we found that analysing simulations in an observational way brings results in much better agreement with observations. This suggests that observations inevitably suffer from biases, at least in the sense that photometric images might not be able to catch in detail the kinematic properties of a galaxy.

Another important limitation is that different codes can sometimes predict different results, even for a given dark matter halo. We have made a detailed comparison of 13 hydrodynamical codes, and found that most differences can be attributed to differences in the implementation of feedback processes. Our results indicate that more sophisticated models of feedback need to be introduced, to be able to better understand the effects of feedback processes on the star formation, gas content and morphology of galaxies.

Studies of galaxy formation in a cosmological context have been very important during the last years, and have helped to test our theories of galaxy formation. They have shown successful in reproducing many of the observed properties of galaxies and, more important, they have helped to start understanding the effects of feedback processes on the evolution of the baryonic components. During the next years, simulations of larger samples of galaxies, runs with higher resolution, and more sophisticated modelling of feedback processes will be crucial to overcome the open problems in this field.

*Acknowledgements.* CS thanks the Organizing Committee for the invitation to give a review talk on this topic.

## References

- Abadi, M.G., Navarro, J.F., Steinmetz, M., Eke, V.R.: 2003, *ApJ* 597, 21
- Agertz, O., et al.: 2007, *MNRAS* 380, 963
- Agertz, O., Teyssier, R., Moore, B.: 2011, *MNRAS* 410, 1391
- Boylan-Kolchin, M., Springel, V., White, S.D.M., Jenkins, A., Lemson, G.: 2009, *MNRAS* 398, 1150
- Brooks, A.M., Governato, F., Quinn, T., Brook, C.B., Wadsley, J.: 2009, *ApJ* 694, 396
- Bruzual, G., Charlot, S.: 2003, *MNRAS* 344, 1000
- Ceverino, D., Klypin, A.: 2009, *ApJ* 695, 292
- Gadotti, D.A.: 2008, *MNRAS* 384, 420
- Governato, F., et al.: 2004, *ApJ* 607, 688
- Governato, F., Willman, B., Mayer, L., et al.: 2007, *MNRAS* 374, 1479
- Haardt, F., Madau, P.: 1996, *ApJ* 461, 20
- Jonsson, P.: 2006, *MNRAS* 372, 2
- MacArthur, L.A., Courteau, S., Bell, E., Holtzman, J.A.: 2004, *ApJS* 152, 175
- MacArthur, L.A., González, J.J., Courteau, S.: 2009, *MNRAS* 395, 28
- Mayer, L., Governato, F., Kaufmann, T.: 2008, *Adv. Sci. Lett.* 1, 7
- Navarro, J.F., Benz, W.: 1991, *ApJ* 380, 320
- Navarro, J.F., Steinmetz, M.: 1997, *ApJ* 478, 13
- Navarro, J.F., Steinmetz, M.: 2000, *ApJ* 538, 477
- Okamoto, T., Eke, V.R., Frenk, C.S., Jenkins, A.: 2005, *MNRAS* 363, 1299
- Rasera, Y., Teyssier, R.: 2006, *A&A* 445, 1
- Sawala, T., Scannapieco, C., Maio, U., White, S.: 2010, *MNRAS* 402, 1599
- Sawala, T., Guo, Q., Scannapieco, C., Jenkins, A., White, S.: 2011, *MNRAS* 413, 659
- Scannapieco, C., Tissera, P.B., White, S.D.M., Springel, V.: 2005, *MNRAS* 364, 552
- Scannapieco, C., Tissera, P.B., White, S.D.M., Springel, V.: 2006, *MNRAS* 371, 1125
- Scannapieco, C., Tissera, P.B., White, S.D.M., Springel, V.: 2008, *MNRAS* 389, 1137
- Scannapieco, C., White, S.D.M., Springel, V., Tissera, P.B.: 2009, *MNRAS* 396, 696
- Scannapieco, C., Gadotti, D.A., Jonsson, P., White, S.D.M.: 2010, *MNRAS* 407, L41
- Scannapieco, C., White, S.D.M., Springel, V., Tissera, P.B.: 2011, *MNRAS* 417, 154
- Scannapieco, C., Wadepuhl, M., Parry, O.H., et al.: 2012, *astro-ph/1112.0315*
- Springel, V.: 2005, *MNRAS* 364, 1105
- Springel, V., Hernquist, L.: 2003, *MNRAS* 339, 289
- Springel, V., et al.: 2008, *MNRAS* 391, 1685
- Stinson, G., Seth, A., Katz, N., Wadsley, J., Governato, F., Quinn, T.: 2006, *MNRAS* 373, 1074
- Stinson, G.S., Bailin, J., Couchman, H., et al.: 2010, *MNRAS* 408, 812
- Tissera, P.B., White, S.D.M., Pedrosa, S., Scannapieco, C.: 2010, *MNRAS* 406, 922
- Tissera, P.B., White, S.D.M., Scannapieco, C.: 2012, *MNRAS* 420, 255